The Journal of Immunology

Allele- and Locus-Specific Recognition of Class I MHC Molecules by the Immunomodulatory E3-19K Protein from Adenovirus

Hong Liu, Jie Fu and Marlene Bouvier

J Immunol 2007; 178:4567-4575; ;
doi: 10.4049/jimmunol.178.7.4567
http://www.jimmunol.org/content/178/7/4567

The Journal of Immunology is published twice each month by
The American Association of Immunologists, Inc.,
1451 Rockville Pike, Suite 650, Rockville, MD 20852

Print ISSN: 0022-1767 Online ISSN: 1550-6606.

Allele- and Locus-Specific Recognition of Class I MHC Molecules by the Immunomodulatory E3-19K Protein from Adenovirus[1]

Hong Liu,[2] Jie Fu,[2] and Marlene Bouvier[3]

The E3-19K protein from human adenoviruses (Ads) retains class I MHC molecules in the endoplasmic reticulum. As a consequence, the cell surface expression of class I molecules is suppressed, allowing Ads to evade immune surveillance. Using native gel electrophoresis, gel filtration chromatography, and surface plasmon resonance, we show that a soluble form of the Ad type 2 (Ad2) E3-19K protein associates with HLA-A and -B molecules; equilibrium dissociation constants were in the nanomolar range and ~2.5-fold higher affinity for HLA-A (-A*0201, -A*0301, -A*1101, -A*3301, and -Aw*6801) relative to HLA-B (-B*0702 and -B*0801) molecules. Among the alleles of the HLA-A locus examined, HLA-A*3101 associated ~15-fold less avidly with soluble E3-19K. Soluble E3-19K interacted only very weakly with HLA-Cw*0304, and no interaction with HLA-Cw*0401 could be detected under identical conditions. Site-directed mutagenesis and flow cytometry demonstrated that MHC residue 56 plays a critical role in the association and endoplasmic reticulum retention of HLA-A molecules by E3-19K. This delineates the spatial environment around residue 56 as a putative E3-19K interaction surface on class I molecules. Overall, our data imply that a link may exist between host genetic factors and the susceptibility of individuals to Ad infections. ***The Journal of Immunology,*** **2007, 178: 4567–4575.**

Human adenoviruses (Ads)[4] cause infections that are responsible for a variety of respiratory, gastrointestinal, ocular, and urinary tract diseases (1). Although a primary infection by Ads elicits host immune responses in which $CD8^+$ CTLs play an important role, these responses are usually insufficient to clear the virus. Such viral persistence in the context of a fully primed immune system underscores the ability of Ads to subvert host antiviral immune responses.

The Ad genome includes a number of genes that encode immunomodulatory proteins (reviewed in Refs. 2 and 3). Some of these proteins act by down-regulating the cell surface expression of class I MHC molecules. For example, the highly oncogenic Ad12 encodes proteins in the early region (E) 1A (E1A) (4) that repress transcription of the class I H chain gene (4). Evidence has also been provided that E1A proteins repress the transcription of genes encoding class I assembly proteins such as TAP1 and TAP2 (5). The genome of some Ads encodes the E3-19K protein that associates with class I molecules in the endoplasmic reticulum (ER) and prevents their transport to the cell surface (6–9). E3-19K was also shown to bind to TAP, an association that likely prevents TAP from interacting with the class I assembly protein tapasin (10). Other *E3*-encoded immunomodulatory proteins have been characterized; these proteins were, however, shown to function through mechanisms other than class I cell surface down-regulation (reviewed in Ref. 11).

A clear role for E3-19K in down-regulating class I cell surface expression and in suppressing the susceptibility to lysis by $CD8^+$ CTLs has been demonstrated in Ad-infected cells (6, 7, 12–15). For example, class I molecules can be found on the surface of cells infected by Ad mutants that lack the expression of E3-19K (16). The same Ad mutants were shown to cause enhanced pathological cellular responses to pulmonary infection in cotton rats (16). This apparent critical role played by E3-19K in subverting antiviral immune responses likely underlies the ability of Ads to establish persistent infection in humans.

Two distinct features of E3-19K are responsible for targeting and retaining class I molecules in the ER: the ER lumenal domain of E3-19K associates with the ER lumenal domain of class I molecules (7, 17–24), and the ER retention motif in the cytosolic domain of E3-19K blocks the transport of class I molecules to the cell surface (21, 22). An analysis of immunoprecipitates from Ad2-, Ad5-, and Ad19a-infected mammalian cells suggested that E3-19K displays differential associations with class I molecules (17, 23–25); E3-19K appeared to associate more avidly with HLA-A2 and -B7 than either HLA-A3 and -Aw69, which, in turn, are both more strongly targeted by E3-19K than HLA-Aw68 and -B27. This lead to the suggestion that the pathogenicity of Ads in humans may be dependent on the class I HLA gene products of the infected individuals, with persistent infections occurring preferentially in individuals expressing alleles that strongly interact with E3-19K (2, 23).

In the present study, we conducted a direct analysis of the interaction between the ER lumenal domains of Ad2 E3-19K and several class I molecules of the HLA-A, -B, and -C loci to characterize the binding specificities of soluble E3-19K. Using native gel electrophoresis, gel filtration chromatography, site-directed mutagenesis, surface plasmon resonance (SPR), and flow cytometry, we show that soluble E3-19K (hereafter referred to as E3-19K) associates with HLA-A and -B molecules; interaction with HLA-C molecules is only very weak. Overall, this work provides insights into how a natural polymorphism in *MHC* modulates the

School of Pharmacy, University of Connecticut, Storrs, CT 06269

Received for publication July 6, 2006. Accepted for publication January 22, 2007.

The costs of publication of this article were defrayed in part by the payment of page charges. This article must therefore be hereby marked *advertisement* in accordance with 18 U.S.C. Section 1734 solely to indicate this fact.

[1] This project was supported by National Institutes of Health/National Institute of Allergy and Infectious Diseases Grant AI055717 (to M.B.) and in part by a Predoctoral Fellowship from Boehringer-Ingelheim Pharmaceuticals (to H.L.).

[2] H.L. and J.F. contributed equally to this work.

[3] Address correspondence and reprint requests to Dr. Marlene Bouvier, School of Pharmacy, 69 N. Eagleville Road, U-3092, Storrs, CT 06269. E-mail address: marlene.bouvier@uconn.edu

[4] Abbreviations used in this paper: Ad, adenovirus; β_2m, β_2-microglobulin; E, early region; ER, endoplasmic reticulum; RT, reverse transcriptase; RU, resonance unit; SPR, surface plasmon resonance.

immunomodulatory function of E3-19K and may contribute to the pathogenesis of Ads in vivo.

Materials and Methods

Cell line and mAbs

The human B lymphoblastoid cell line Hmy2.C1R (C1R) (a gift from Dr. P. Cresswell, Yale University School of Medicine, New Haven, CT) was grown in IMDM containing L-glutamine (2 mM), penicillin (100 IU/ml), and streptomycin (100 μg/ml) and supplemented with 10% FBS. W6/32 (Abcam), anti-HLA-A31 (One Lambda), and anti-HLA-A33 (One Lambda) were used as mAbs; FITC-conjugated rat anti-mouse IgG (eBioscience) and FITC-conjugated goat anti-mouse IgM (Jackson ImmunoResearch Laboratories) were used as secondary Abs.

Cloning and expression

Expression plasmids for the ER lumenal domains of the HLA-A*0301, -A*1101, -A*3101, -A*3301, -Aw*6801, and -B*0702 H chains were described previously (26, 27). Plasmids for expression of the ER lumenal domains of the HLA-A*0201, -B*0801, -Cw*0304, and -Cw*0401 H chains were gifts of Drs. Y. Jones (University of Oxford, Oxford, U.K.), P. Sun (National Institutes of Health, Rockville, MD), and D. Wiley (deceased). The cDNAs encoding the ER lumenal domain of the HLA-A*3101R56G and -A*3301G56R H chains were generated by PCR using the QuikChange site-directed mutagenesis approach (Stratagene) and the plasmids of the HLA-A*3101 and -A*3301 H chains as templates. Plasmids harboring the correct DNA sequence for the HLA-A*3101R56G and -A*3301G56R H chains were transformed into competent BL21(DE3)pLysS cells. The expression of H chains and the β_2-microglobulin (β_2m) was conducted in *Escherichia coli*; proteins were isolated from the cell pellets as inclusion bodies that were washed and solubilized (28).

The cDNAs of full-length HLA-A*3101 and -A*3301 H chains (International Histocompatibility Working Group, Seattle, WA) were inserted into the *Hin*dIII and *Not*I restriction sites of the pcDNA3.1 vector (Invitrogen Life Technologies). The cDNA of the full-length HLA-A*3301G56R H chain was generated by QuikChange (Stratagene) using the plasmid pcDNA3.1/HLA-A*3301 as template. All plasmids were linearized with *Bgl*II followed by transfection into C1R cells by electroporation. Transfectants were incubated in IMDM supplemented with 10% FBS for 48 h followed by plating into 24-well plates. Selection of transfectants was initiated with 600 μg/ml G418 (Calbiochem). After 20 days, drug-resistant transfectants were expanded and maintained in 300 μg/ml G418. Class I cell surface expression was analyzed by flow cytometry (see below).

The ER lumenal domain (residues 1–100) of Ad2 E3-19K with a C-terminal His_6 tag sequence was expressed and purified as described previously (20).

Viruses and infection

Ad2 and Ad2$^+$ND1 (entire *E3* region deleted (29)) (gifts of Dr. P. Flomenberg, Thomas Jefferson University, Philadelphia, PA) were grown in HeLa S3 cells in DMEM (HyClone) supplemented with 10% FBS. Cells were harvested at 48–72 h postinfection when a cytopathic effect was observed. Cells were subjected to three freeze/thaw cycles to release viral particles. Cellular debris was removed by centrifugation and the supernatants containing the viruses were purified using the Adeno-X virus purification kit (Clontech). HLA-A*3101, -A*3301, and -A*3301G56R transfectants (2.5×10^6 cells) were infected with Ad2 and Ad2$^+$ND1 at an estimated multiplicity of infection in the range of 60–100 in serum-free IMDM. After 1 h, 4 ml of IMDM containing 10% FBS was added to the cells. Mock infections were conducted in an identical manner. Mock- and Ad-infected transfectants were harvested at 24 h postinfection. Class I cell surface expression was analyzed by flow cytometry (see below).

Biotinylation of β_2m

Refolded β_2m (118 μM) was biotinylated for 3 h at room temperature with a 20-fold molar excess of *N*-hydroxysuccinimidobiotin (Sigma-Aldrich). The reaction was quenched by the addition of 1 M Tris (pH 7.5).

Assembly of soluble class I molecules

The refolding of soluble class I molecules was initiated by diluting urea-solubilized inclusion bodies of a class I H chain (1 μM) and β_2m (2 μM) in the presence of a synthetic peptide (10 μM) in an oxidative refolding buffer (28). Biotinylated class I molecules were assembled using biotinylated β_2m (2 μM). Class I molecules were purified on a Superdex 200 HR 10/30 column in 20 mM Tris and 150 mM NaCl (pH 7.5).

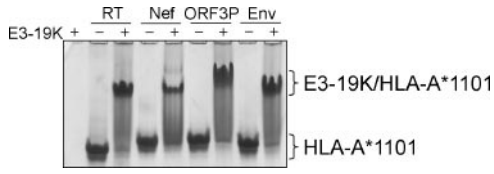

FIGURE 1. Interaction between E3-19K and HLA-A*1101 molecules loaded with different peptides. E3-19K (14 μg) and HLA-A*1101 molecules (20 μg) (2:1 molar ratio) were incubated on ice in 20 mM Tris and 150 mM NaCl (pH 7.5) for 30 min followed by the addition of loading buffer (50 mM Tris, 0.1% bromophenol blue, and 10% glycerol (pH 6.8)). Peptides were RT (AIFQSSMTK), Nef (QVPLRPMTYK), ORF3P (MSLQRQFLR), and Env (RVLKQVTEK). The native gel (10%) was run at 4°C in 25 mM Tris and 200 mM glycine (pH 8.3). Because the isoelectric point of E3-19K (pI 8.85) is higher than the pH of the running buffer, uncomplexed E3-19K does not penetrate into the gel under these conditions. Differences in isoelectric points caused uncomplexed HLA-A*1101 molecules to migrate differently in native gel.

Flow cytometry

HLA-A*3101, -A*3301, and -A*3301G56R transfectants were analyzed and sorted by flow cytometry on a FACSCalibur device (BD Biosciences). Cells were washed twice with FACS buffer (PBS containing 1% BSA and 0.1% NaN_3). After blocking with rabbit IgG (Sigma-Aldrich), cells were incubated at 4°C with the W6/32 mAb for 45 min, washed three times, and incubated with FITC-conjugated IgG for 45 min. For Ad- and mock-infected transfectants, cells were incubated with anti-A31 (for HLA-A*3101) and anti-A33 (for HLA-A*3301 and -A*3301G56R) and the FITC-conjugated IgM, followed by fixing in 1% paraformaldehyde in the dark for 10 min. Cells were analyzed for class I cell surface expression by gating to exclude dead cells. All data are representative of three independent experiments. Data analysis was performed with FlowJo software (Tree Star).

Surface plasmon resonance

SPR experiments were conducted at 20°C using a BIAcore 3000 biosensor in HBS-EP (10 mM HEPES, 150 mM NaCl, 3 mM EDTA, and 0.005% surfactant P20 (pH 7.4)). Biotinylated class I molecules were immobilized on a streptavidin-coated surface to ~500 resonance units (RU) at a flow rate of 10 ml/min. Uncoupled streptavidin sites were blocked by biotin (30 ml/min for 1 min). Identical conditions were used for the control flow cell. Solutions of E3-19K (in the range 3.125–2000 nM) were injected through the flow cells (60 ml/min for 4 min) and responses (with control responses automatically subtracted) were recorded. The regeneration of binding surfaces was conducted in HBS-EP. Blank injections consisting of HBS-EP were included among the samples; the averaged responses of blanks were removed from the entire data set to eliminate systematic artifacts. Responses obtained after immobilizing HLA-A*1101 to 500, 1000, and 2000 RU at flow rates of 5, 15, and 75 ml/min were unaffected by mass transfer. Kinetics dissociation constants were derived by globally fitting the association and dissociation phases of the sensorgrams in the BIAevaluation software (version 3.0; Biacore) assuming a 1:1 Langmuir binding model (this assumption is valid; see Ref. 20). Equilibrium dissociation constants were obtained by fitting plots of steady-state association responses vs the E3-19K concentration based on a 1:1 Langmuir binding model. Residual plots were carefully inspected and showed noise levels of ± ~3 RU.

Native gel band-shift assay

E3-19K (14 μg) and class I molecules (20 μg) (2:1 molar ratio) were incubated in 20 mM Tris and 150 mM NaCl (pH 7.5) on ice for 30 min. Incubation mixtures were assayed by electrophoresis on a native polyacrylamide gel (10%) at 4°C in 25 mM Tris and 200 mM glycine (pH 8.3). Proteins were visualized with Coomassie blue staining.

Gel filtration chromatography

Samples of E3-19K, class I molecules, and E3-19K/class I complexes were analyzed at 10°C on a Superdex 200 HR 10/30 column in 20 mM Tris and 150 mM NaCl (pH 7.5).

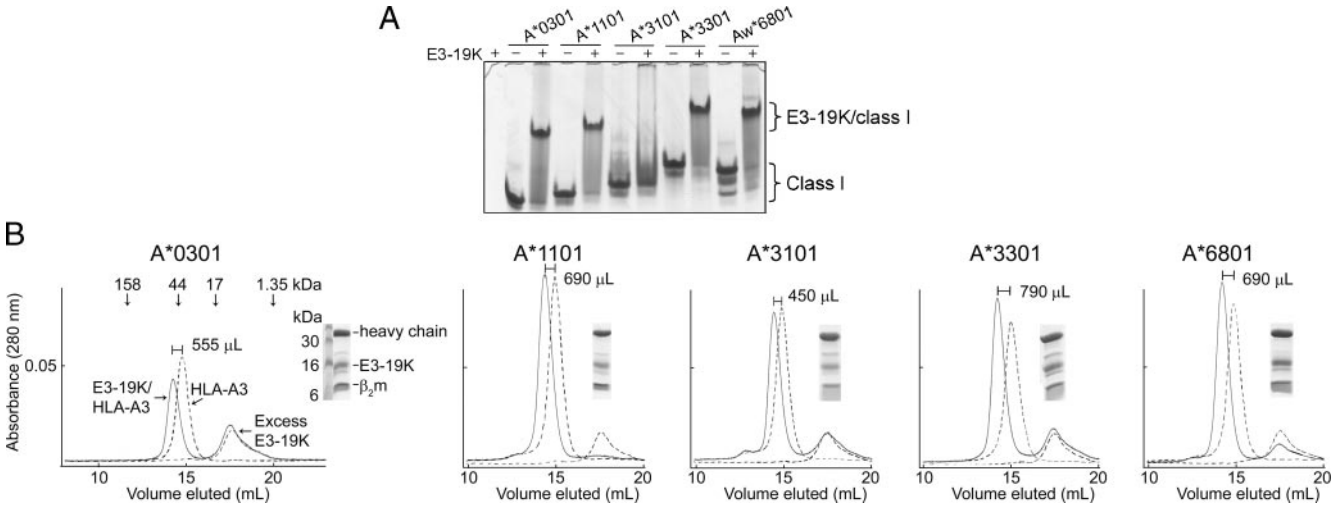

FIGURE 2. Interaction between E3-19K and HLA-A3-like molecules. *A*, E3-19K (14 μg) and HLA-A3-like molecules (20 μg) (2:1 molar ratio) were incubated as described in Fig. 1. Peptides were RT (AIFQSSMTK) for HLA-A*0301, -A*1101, -A*3101, and -Aw*6801 and ORF3P (MSLQRQFLR) for HLA-A*3301. The native gel (10%) was run as described in Fig. 1. *B*, Samples of E3-19K (83 μg) and HLA-A3-like molecules (147 μg) (2:1 molar ratio) were incubated as described in Fig. 1 and loaded onto a Superdex 200 HR 10/30 column at 10°C in 20 mM Tris and 150 mM NaCl (pH 7.5). The chromatograms (solid lines) show major peaks eluting earlier than uncomplexed HLA-A3-like molecules and E3-19K (dashed lines). Differences in elution volumes between E3-19K/class I complexes and uncomplexed class I molecules are indicated. Calibration markers are indicated at the top of the HLA-A*0301 chromatogram. The main fraction for each mixture was analyzed by electrophoresis on a SDS-polyacrylamide gel (15%) (*inset*).

Peptide synthesis

Peptides were synthesized at the Microcore Facility of Tufts University (Boston, MA).

Results

*Bound peptides are unlikely to be integral components of the interaction surface between E3-19K and HLA-A*1101*

In previous studies (20) we showed that E3-19K forms a stable complex with HLA-A*1101 loaded with the Nef peptide (QVPL RPMTYK) (30). In the present study we extended this analysis by including the following nonameric peptides: reverse transcriptase (RT) (AIFQSSMTK) from HIV-1 (30), ORF3P (MSLQRQFLR) from tyrosinase-related protein-2 (31), and Env (RVLKQVTEK) from HIV-1 (30). E3-19K was incubated with HLA-A*1101 molecules (2:1 molar ratio) on ice followed by native gel electrophoresis (Fig. 1). Results show that E3-19K associated with all of the HLA-A*1101 molecules as indicated by the presence of intense new bands as well as the disappearance of the bands corresponding to uncomplexed HLA-A*1101 molecules. Given the distinct nature of peptides tested, these results suggest that bound peptides are unlikely to be integral components of the E3-19K interaction surface on class I molecules as they are in complexes between T cell and Ig-like NK receptors and class I.

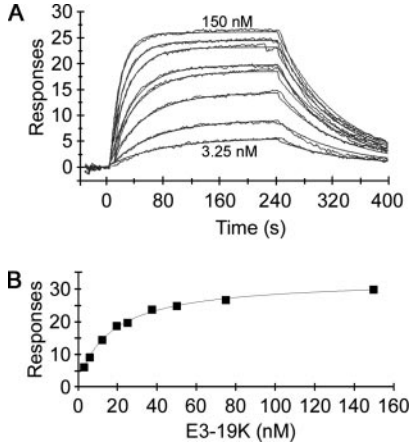

FIGURE 3. Analysis of interaction between E3-19K and HLA-A*0301 by surface plasmon resonance. *A*, Solutions of E3-19K (3.25–150 nM) were injected through the control (immobilized biotin) and sample flow cells. Association and dissociation time courses were recorded with the responses from the control cell being automatically subtracted. Solid lines through the sensorgrams were generated from globally fitting the data to a 1:1 Langmuir binding model, yielding a kinetics dissociation constant of 13.9 ± 3.1 nM. *B*, A plot of binding responses measured at equilibrium vs concentration of E3-19K. The solid line through the data points represents a nonlinear fit of the 1:1 Langmuir binding isotherm. The equilibrium dissociation constant was found to be 14.9 ± 4.7 nM. All measurements were recorded at 20°C on a streptavidin-coated surface.

Interaction between E3-19K and class I molecules of the HLA-A3 superfamily

Interaction between E3-19K and HLA-A3-like molecules (HLA-A*0301, -A*1101, -A*3101, -A*3301, and -Aw*6801) were examined by native gel electrophoresis under identical conditions as

Table I. *Summary of dissociation constants*[a]

Immobilized[b]	K_d (nM) Kinetics	K_d (nM) Equilibrium
A*0201	10.9 ± 0.2	12.8
A*0301	13.9 ± 3.1	14.9 ± 4.7
A*1101	14.5 ± 2.1	15.5 ± 2.8
A*3101	ND[c]	255 ± 21
A*3301	17.6 ± 2.7	18.3 ± 3
Aw*6801	17.3 ± 0.4	17.3 ± 1.7
A*3101R56G	18.3 ± 2.3	18.6 ± 4.5
A*3301G56R	ND[c]	630 ± 170
B*0702	ND[c]	41.6
B*0801	ND[c]	39.7 ± 4.3
Cw*0304	NB[d]	NB[d]
Cw*0401	NB[d]	NB[d]

[a] Determined in duplicate by surface plasmon resonance at 20°C (±SD).
[b] See text for peptide sequences.
[c] Could not be determined reliably.
[d] No binding detected with E3-19K injected up to 2 μM.

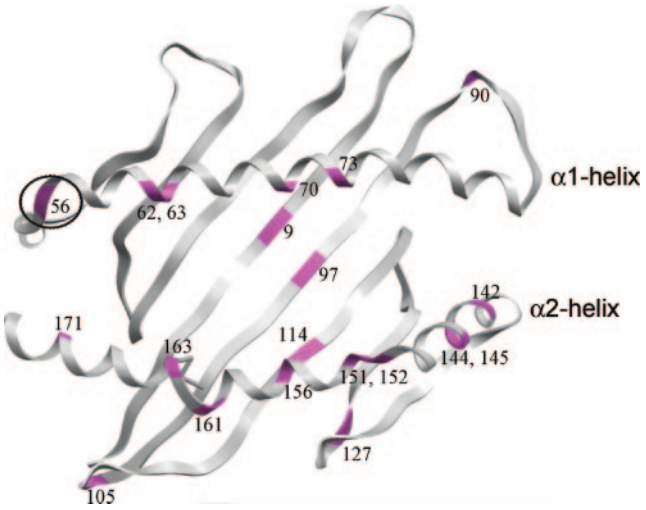

FIGURE 4. Natural polymorphism in the HLA-A3 superfamily. Polymorphic residues (pink) in the peptide-binding groove (residues 1–175) between HLA-A*0301, -A*1101, -A*3101, -A*3301, and -Aw*6801. Residue 56 (circled) is the sole polymorphic residue that is uniquely distinct in the HLA-A*3101 H chain (residues 1–275). MHC residues are mapped in the structure of HLA-A*1101/Nef (43), with Nef omitted.

those described above. HLA-A3-like molecules were refolded with RT except for HLA-A*3301, which was refolded with ORF3P (RT cannot promote the assembly of HLA-A*3301). This difference in bound peptides is unlikely to influence interaction with E3-19K based on the above findings. Analysis of incubation mixtures (Fig. 2*A*) showed that E3-19K forms a complex with HLA-A*0301, -A*1101, -A*3301, and -Aw*6801 as indicated by strong bands that migrated at different positions relative to uncomplexed proteins. In previous studies with HLA-A*1101 (20), we confirmed by N-terminal amino acid sequencing that each component of the complex is present in the new band, i.e., E3-19K, the HLA-A*1101 H chain, β_2m, and the peptide. Interestingly, the incubation of E3-19K with HLA-A*3101 under identical conditions failed to generate an intense band. Instead, the mixture of E3-19K and HLA-A*3101 lead to a protein smear as well as a faint band corresponding to uncomplexed HLA-A*3101. Because all mixtures had identical concentrations of E3-19K and HLA-A3-like molecules, the results are consistent with the E3-19K/HLA-A*3101 complex undergoing dissociation during electrophoresis owing to weaker interaction. Overall, results from the native gel indicate that E3-19K associates readily with HLA-A*0301, -A*1101, -A*3301, and -Aw*6801, but less avidly with -A*3101.

Mixtures of E3-19K and HLA-A3-like molecules were also analyzed by gel filtration chromatography (Fig. 2*B*). Chromatograms (Fig. 2*B*, solid lines) show major peaks eluting from the gel filtration column earlier than those of uncomplexed HLA-A3-like molecules and E3-19K (dashed lines). Interestingly, these major peaks eluted noticeably earlier (relative to uncomplexed class I molecules) for HLA-A*0301, -A*1101, -A*3301, and -Aw*6801 (681 μl on average) than for -A*3101 (450 μl). These results are consistent with complexes between E3-19K and HLA-A*0301, -A*1101, -A*3301, and -Aw*6801 being more strongly associated than the E3-19K/-A*3101 complex during elution through the column. Major fractions were collected and analyzed by SDS-PAGE (Fig. 2*B*, *insets*) and the results confirmed the presence of the H chain, E3-19K, and β_2m. Overall, results from gel filtration chromatography showed that E3-19K interacts more avidly with HLA-A*0301, -A*1101, -A*3301, and -Aw*6801 than with -A*3101. This is in agreement with conclusions from the native gel (Fig. 2*A*).

Measurements of affinities between E3-19K and HLA-A3-like molecules

A quantitative analysis of interaction between E3-19K and HLA-A3-like molecules was conducted by SPR. Biotinylated HLA-A3-like molecules, loaded with the same peptides as those used above, were immobilized on a streptavidin-coated surface. Solutions of E3-19K were injected through the control (immobilized biotin) and sample flow cells, and time courses of the association and dissociation phases were recorded at 20°C. The sensorgrams were globally fitted in the BIAevaluation software based on a 1:1 Langmuir binding model as exemplified in Fig. 3*A* for HLA-A*0301. Optimal fittings yielded kinetics dissociation constants (K_d) of ~16 nM for all HLA-A3-like molecules (Table I). A typical plot of the dependence of association responses measured at equilibrium on concentrations of E3-19K is presented in Fig. 3*B* for HLA-A*0301. Optimal fits of the data yielded equilibrium dissociation constants (K_d) of ~17 nM for HLA-A*0301, -A*1101, -A*3301, and -Aw*6801 (Table I). These values are in excellent agreement with those obtained from kinetics analysis. A significantly higher equilibrium dissociation constant, K_d = 255 nM, was measured for HLA-A*3101 (Table I); this represents ~15-fold decrease in affinity relative to other HLA-A3-like molecules. These differential associations are entirely consistent with results from native gel and gel filtration chromatography (Fig. 2). Overall, measured affinities between E3-19K and HLA-A3-like molecules show that HLA-A*3101 undoubtedly possesses distinct features that allow it to be more refractory to recognition by E3-19K.

Analysis of natural polymorphism in the HLA-A3 superfamily

To gain insights into the molecular basis of these differential associations, we compared amino acid sequences of the ER lumenal domains (residues 1–275) of the HLA-A*0301, -A*1101, -A*3101, -A*3301, and -Aw*6801 H chains. The analysis revealed that the vast majority of polymorphic residues are located in the peptide-binding groove (residues 1–175) (Fig. 4 and Table II) (26): on the floor, residues 9, 97, and 114; on solvent-exposed loops, residues 90, 105, and 127; and on the α-helices, residues 56, 62, 63, 70, 73, 142, 144, 145, 151, 152, 156, 161, 163, and 171. Only seven polymorphic residues (residues 184, 193, 194, 207,

Table II. *Analysis of natural polymorphism in the HLA-A3 superfamily*

	Residues																			
Alleles	9	56	62	63	70	73	90	97	105	114	127	142	144	145	151	152	156	161	163	171
A*0301	F	G	Q	E	Q	T	A	I	S	R	N	I	K	R	H	E	L	D	T	Y
A*1101	Y	G	Q	E	Q	T	D	I	P	R	N	I	K	R	H	A	Q	E	R	Y
A*3101	T	R[a]	Q	E	H	I	A	M	S	Q	N	I	Q	R	R	V	L	E	T	Y
A*3301	T	G	R	N	H	I	A	M	S	Q	N	I	Q	R	R	V	L	E	T	H
Aw*6801	Y	G	R	N	Q	T	A	M	S	R	K	T	K	H	H	V	W	E	T	Y

[a] Sole polymorphic residue that is uniquely distinct in HLA-A*3101.

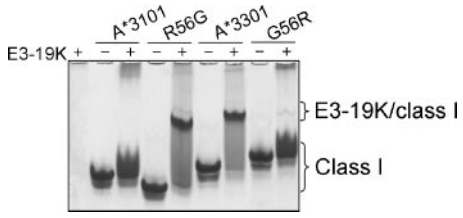

FIGURE 5. MHC residue 56 modulates the interaction with E3-19K. E3-19K (14 μg) and class I molecules (20 μg) (2:1 molar ratio) were incubated as described in Fig. 1. The native gel (10%) was run as described in Fig. 1.

245, and 253) were identified in the membrane-anchoring α3 domain (omitted in Fig. 4 and Table II). Perhaps most significant, among all polymorphic sites in the ER lumenal domain, residue 56 was identified as the sole residue that is uniquely distinct in HLA-A*3101 (Table II). Indeed, while HLA-A*0301, -A*1101, -A*3301, and -Aw*6801 carry Gly^{56}, HLA-A*3101 carries Arg^{56}. This polymorphism at position 56 is particularly striking because it is occupied by a small neutral Gly residue in the strongly associating HLA-A*0301, -A*1101, -A*3301, and -Aw*6801 alleles but by a large positively charged Arg residue in the more weakly associating HLA-A*3101 allele. Importantly, HLA-A*0201, another allele of the HLA-A locus carrying Gly^{56}, also strongly associates with E3-19K (Table I). Overall, this analysis provides a strong rationale for investigating the role of MHC residue 56 in modulating the interaction with E3-19K.

MHC residue 56 modulates interaction between E3-19K and HLA-A3-like molecules

To assess the impact of the natural polymorphism at position 56 in the class I H chain on the interaction with E3-19K, an Arg^{56}-to-Gly^{56} (R56G) mutation was introduced in the HLA-A*3101 H chain by site-directed mutagenesis. Similarly, a Gly^{56}-to-Arg^{56} (G56R) mutation was introduced in the highly homologous HLA-A*3301 H chain (note that there are only four polymorphic residues between the HLA-A*3101 and -A*3301 H chains (residues 1–275)). Interaction between E3-19K and HLA-A*3101R56G and -A*3301G56R (both loaded with ORF3P) was monitored by native gel electrophoresis (Fig. 5). The results clearly show that the incubation of E3-19K with HLA-A*3101R56G yielded a strong band on the gel. In marked contrast, the incubation of E3-19K with HLA-A*3301G56R failed to generate a strong band at the positions of other complexes. Instead, a protein smear similar to that observed for the mixture of E3-19K and HLA-A*3101 (see Fig. 2*A*) was apparent. Thus, together these results demonstrate that the mutation of residue 56 in the HLA-A*3101 and -A*3301 H chains affected the interaction with E3-19K; whereas the R56G mutation in HLA-A*3101 promoted interaction, the G56R mutation in HLA-A*3301 significantly diminished interaction. It is possible that the bulky, positively charged Arg suppresses complex formation by creating charge repulsion and/or steric hindrance effects at the E3-19K binding site. Together, these results strongly suggest that MHC residue 56 modulates interaction between E3-19K and HLA-A3-like molecules.

SPR was used to quantitate the interaction between E3-19K and HLA-A*3101R56G and -A*3301G56R (both loaded with ORF3P). Analysis of the sensorgrams (Table I) showed that the R56G mutation in the HLA-A*3101 H chain restored interaction with E3-19K (K_d = 18.6 nM) to the same level as the strongly associating HLA-A*0301, -A*1101, -A*3301, and -Aw*6801 alleles. In contrast, the G56R mutation in the HLA-A*3301 H chain yielded K_d = 630 nM (Table I); this represents an ~35-fold decrease in affinity relative to wild-type HLA-A*3301. These results are consistent with the behavior of these complexes on native gel (Fig. 5); the weaker E3-19K/HLA-A*3101 and E3-19K/HLA-A*3301G56R complexes yielded a protein smear rather than a new band. Thus, site-directed mutagenesis convincingly showed that MHC residue 56 critically influences the avidity of interaction between E3-19K and HLA-A3-like molecules.

MHC residue 56 influences the cell surface expression of HLA-A3-like molecules

To determine whether the differential recognition of HLA-A*3101 and -A*3301 by E3-19K has functional consequences, Ad2-infected C1R cells stably expressing HLA-A*3101 and -A*3301 were analyzed by flow cytometry (Fig. 6, *A* and *B*, respectively). As a control, mock treatments of transfected cells were also performed. Analysis of the data (Table III) show that, relative to mock-infected cells, the cell surface expression of HLA-A*3101 and -A*3301 in Ad2-infected cells was 85.2 and 24.5%, respectively. These results indicate that HLA-A*3101 is readily expressed on the surface of Ad-infected cells while HLA-A*3301 is significantly down-regulated. In fact, the level of -A*3101 cell surface expression approaches that on the surface of mock-infected

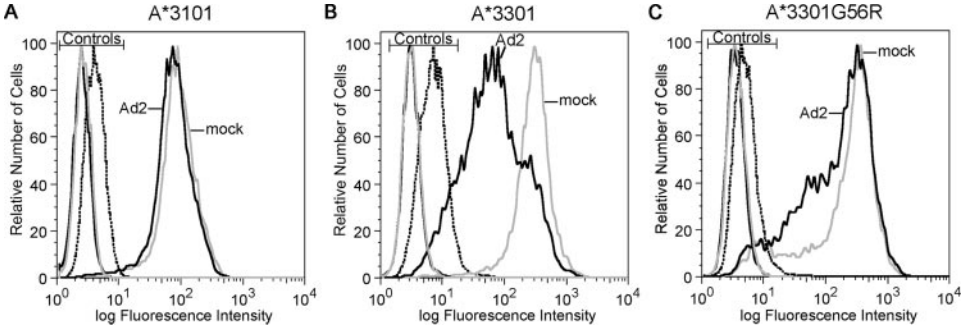

FIGURE 6. MHC residue 56 influences the immunomodulatory function of E3-19K. The expression of HLA-A*3101 (*A*), HLA-A*3301 (*B*), and HLA-A*3301 G56R (*C*) on the surface of C1R cells was analyzed by flow cytometry at 24 h postinfection with Ad2 (black lines). The expression of HLA-A*3101, -A*3301, and -A*3301G56R on the surface of mock-infected cells (gray lines) is shown in each panel. Controls were untransfected cells incubated with FITC-conjugated IgM (control 1; black line), transfected cells incubated with FITC-conjugated IgM (control 2; gray line), and untransfected cells incubated with either anti-A31 or anti-A33 mAbs followed by FITC-conjugated IgM (control 3; dotted black line). The mean logarithm fluorescence intensity (MFI) of cell surface expression on Ad-infected cells was normalized relative to that on mock-infected cells according to the following equation: percentage of cell surface expression = $((MFI_{Ad\text{-}infected} - MFI_{Control\ 2}) - (MFI_{Control\ 3} - MFI_{Control\ 1}))/((MFI_{mock\text{-}infected} - MFI_{Control\ 2}) - (MFI_{Control\ 3} - MFI_{Control\ 1})) \times 100$. Percentages are reported in Table III. Histograms are representative examples of three independent experiments.

Table III. *Cell-surface expression of class I molecules*[a]

Alleles	Virus		
	Mock	Ad2	Ad2$^+$ND1[b]
A*3101	100	85.2 ± 1.2	104 ± 1.7
A*3301	100	24.5 ± 3.0	107 ± 0.4
A*3301G56R	100	75.9 ± 3.8	121 ± 1.7

[a] Percentage of expression relative to mock infection; see legend of Fig. 7 for how percentages were calculated. Results are from three independent experiments (±SD).
[b] Contains a deletion of the entire *E3* region.

cells (Table III). These results correlate with the binding affinities of these alleles for E3-19K (Table I), the more weakly associating HLA-A*3101 being significantly less retained in the ER than the more strongly binding -A*3301. We also determined whether an Ad2 virus containing a deletion of the entire *E3* region (Ad2$^+$ND1) affects cell surface expression of these alleles. Results show that the cell surface expression of HLA-A*3101 and -A*3301 on Ad2$^+$ND1-infected cells was similar to that on the surface of mock-infected cells (104 and 107%, respectively) (Table III). These results implicate E3-19K in the observed immunomodulatory effects (the possibility that an unidentified *E3*-encoded protein that down-regulates class I cell surface expression may also contribute to our observations cannot be ruled out).

Finally, we examined whether the effect of MHC residue 56 on modulating the interaction with E3-19K also has functional consequences. For this, Ad2-infected CIR cells stably expressing HLA-A*3301G56R were analyzed by flow cytometry (Fig. 6*C*). Results show that, relative to mock-infected cells, the cell surface expression of HLA-A*3301G56R was 75.9% (Table III). This is significantly higher than the cell surface expression of wild-type HLA-A*3301 (24.5%). Thus, the weaker interactions between E3-19K and HLA-A*3301G56R definitely allowed this allele to escape retention by E3-19K. Consistent with the above results, the infection of C1R cells with Ad2$^+$ND1 increased the cell surface expression of HLA-A*3301G56R (Table III). Together, the results from native gel, gel filtration chromatography, SPR, and flow cytometry convincingly demonstrate that MHC residue 56 is key in modulating recognition and ER-retention of HLA-A3-like molecules by E3-19K.

E3-19K interacts with class I molecules of the HLA-B locus but only very weakly with those of the HLA-C locus

To further examine the binding specificities of the ER lumenal domain of E3-19K, we extended our studies to include HLA-B (HLA-B*0702 and -B*0801) and -C (HLA-Cw*0304 and -Cw*0401) molecules. These molecules were respectively refolded with APRTVALTA from HLA-DP (32), FLRGRAYGL from EBV (33), GAVDPLLAL from the importin α-1 subunit (34), and the consensus peptide QYDDAVYKL (35). HLA-B and -C molecules were incubated with E3-19K under identical conditions as those of HLA-A molecules. An analysis of mixtures involving HLA-B*0702 and -B*0801 by native gel electrophoresis (Fig. 7*A*) revealed that neither of these alleles produced new bands. Instead, each mixture generated a protein smear with a faint band corresponding to uncomplexed HLA-B molecules. As discussed above, this suggests weak interaction between E3-19K and HLA-B molecules leading to dissociation of complexes during electrophoresis. Analysis of mixtures involving HLA-Cw*0304 and -Cw*0401 similarly failed to produce new bands on native gel. However, in contrast to HLA-B molecules, intense bands corresponding to uncomplexed HLA-C molecules were visible on the gel; that band was slightly smeary for HLA-Cw*0304. Overall, results from the native gel suggest that the ER lumenal domain of E3-19K interacts with HLA-B molecules and that the interaction with HLA-Cw*0304 is apparently very weak; no interaction with HLA-Cw*0401 could be detected under identical conditions.

Mixtures of E3-19K and HLA-B molecules were also analyzed by gel filtration chromatography (Fig. 7*B*). Results show major peaks (Fig. 7*B*, solid chromatograms) eluting from the gel filtration column earlier than those of uncomplexed HLA-B molecules and E3-19K (dashed chromatograms). Analysis of these major peaks

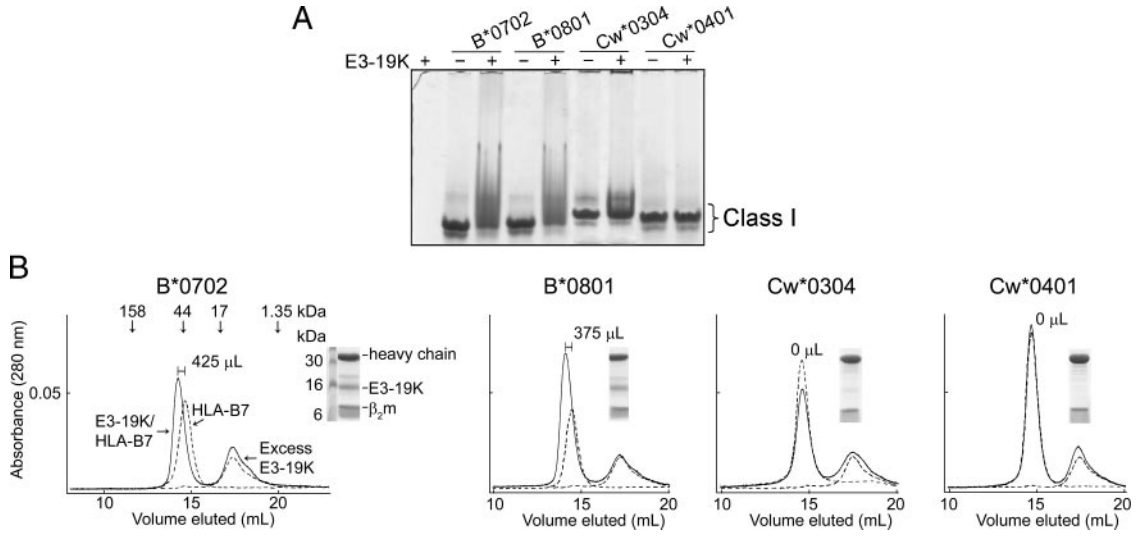

FIGURE 7. Interaction between E3-19K and class I molecules of the HLA-B and -C loci. *A*, E3-19K (14 μg) and class I molecules (20 μg) (2:1 molar ratio) were incubated as described in Fig. 1. HLA-B*0702, -B*0801, -Cw*0304, and -Cw*0401 were respectively refolded with the peptides APRT VALTA, FLRGRAYGL, GAVDPLLAL, and QYDDAVYKL. The native gel (10%) was run as described in Fig. 1. *B*, Samples of E3-19K (83 μg) and the HLA-B and -C molecules (147 μg) (2:1 molar ratio) were incubated as described in Fig. 1 and loaded onto a gel filtration column as described in Fig. 2*B*. The chromatograms (solid lines) show major peaks eluting earlier than the uncomplexed HLA-B molecules and E3-19K (dashed lines); no such fast-eluting peak was observed for HLA-C molecules. Differences in elution volumes between E3-19K/class I complexes and uncomplexed class I molecules are indicated. The main fraction for each mixture was analyzed by electrophoresis on a SDS-polyacrylamide gel (15%) (*inset*).

by SDS-PAGE (*insets*) revealed intense bands corresponding to the H chain, E3-19K, and β_2m. In marked contrast, mixtures of E3-19K and HLA-C molecules (Fig. 7*B*) revealed peaks (solid chromatograms) that eluted at the same position as uncomplexed HLA-C molecules (dashed chromatograms). Analysis of these major peaks by SDS-PAGE (*insets*) reproducibly revealed intense bands for the H chain and β_2m; an extremely faint band corresponding to E3-19K was visible for HLA-Cw*0304, but no E3-19K band could be detected for HLA-Cw*0401. Thus, results from gel filtration chromatography showed that E3-19K interacts with HLA-B molecules, only very weakly with HLA-Cw*0304, and not with HLA-Cw*0401.

These studies were extended to measure the interaction between E3-19K and HLA-B and -C molecules by SPR. Steady-state analysis of sensorgrams of HLA-B molecules yielded K_d values of ~40 nM (Table I). In contrast, no binding could be detected when concentrations of E3-19K as high as 2 μM were injected over immobilized HLA-Cw*0304 and -Cw*0401 (Table I). These results extend those from the native gel and gel filtration chromatography by suggesting that interaction between E3-19K and HLA-Cw*0304 are in the order of $K_d > 2000$ nM. Overall, our data demonstrate that the ER lumenal domain of E3-19K effectively differentiates between polymorphic gene products encoded in the *MHC*.

Discussion

We examined interactions in soluble E3-19K/class I complexes to gain insights into how natural polymorphism in the *MHC* modulates the immunomodulatory function of E3-19K. For this, we first selected alleles of the HLA-A locus (HLA-A*0301, -A*1101, -A*3101, -A*3301, and -Aw*6801) that belong to the HLA-A3 superfamily. Results from native gel electrophoresis, gel filtration chromatography, and SPR showed that the ER lumenal domain of E3-19K forms high-affinity complexes with HLA-A*0301, -A*1101, -A*3301, and -Aw*6801. Kinetics and equilibrium dissociation constants were in the low nanomolar range, which is consistent with the biological function of E3-19K to strongly retain class I molecules in the ER. Our results also revealed that soluble E3-19K displays a significantly lower affinity for HLA-A*3101 (~15-fold decrease). An analysis of interactions between E3-19K and mutants of HLA-A*3101 and -A*3301 showed that this distinctiveness is largely contributed by MHC residue 56. Indeed, the small, neutral Gly^{56} in HLA-A*0301, -A*1101, -A*3301, and -Aw*6801 favors interaction with E3-19K, while the bulky, positively charged Arg^{56} in HLA-A*3101 significantly suppressed interaction with E3-19K. Importantly, within the HLA-A3 superfamily we identified MHC residue 56 as the sole polymorphic residue that is uniquely distinct in the HLA-A*3101 H chain. Thus, the data presented here convincingly demonstrate that natural polymorphism at residue 56 in HLA-A3-like molecules plays a critical role in modulating interaction with E3-19K.

Flow cytometry analysis of HLA-A*3101, -A*3301, and -A*3301G56R showed that the level of expression of these alleles on Ad2-infected cells correlated with their binding affinities for soluble E3-19K. This suggests that the binding specificity displayed by E3-19K toward class I molecules is contributed mostly by interactions involving ER lumenal domains. Although the transmembrane and cytosolic domains may also contribute to interactions within the E3-19K/class I complex (7, 22), our data suggest that these interactions are unlikely to be as specific as those involving ER lumenal domains. Finally, the expression of HLA-A*3101 and -A*3301G56R on the surface of Ad2-infected cells was ~85 and ~75% (Table III), respectively, which is consistent with these alleles being retained to some degree by E3-19K. Alternatively, it is possible that this effect is contributed by E3-19K binding to TAP, an association that was shown to inhibit the incorporation of TAP into the class I assembly complex (10). It was suggested that this second immune evasion mechanism represents a strategy to down-regulate the class I molecules that E3-19K only weakly affects through direct interaction. If so, our data suggest that this secondary mechanism is less effective than that whereby E3-19K associates directly with class I molecules.

To gain insights into whether our findings with HLA-A3-like molecules have broader implications, we compared the amino acid sequences of all reported alleles of the HLA-A locus in the region near MHC residue 56 (IMGT/HLA sequence database; www.ebi.ac.uk/imgt/hla/align.html). Sequence alignments revealed that residues 41–61 (A^{41}SQRMEPRAPWIEQEG^{56}PEYWD^{61}) are highly conserved in all HLA-A alleles. Furthermore, Gly^{56} is absolutely conserved except in a very few alleles that instead carry Arg^{56}, including HLA-A*0107, -A*2619, -A*3404 and most alleles of the HLA-A*30 and -A*31 subtypes. Based on this analysis, it can be concluded that the vast majority of HLA-A alleles are expected to be strongly targeted and retained by E3-19K in the ER of Ad-infected cells. The fact that the MHC residue 56 is located in a highly conserved sequence within the HLA-A locus implicates the spatial region around MHC residue 56 as a putative E3-19K interaction surface. Moreover, because E3-19K/class I complexes form in a 1:1 molar ratio (20), this implies that the spatial region comprising MHC residue 56 is likely to be the sole E3-19K interaction surface on class I molecules. Consistent with our results, a mAb directed at an epitope involving MHC residues 58 and 62 failed to coimmunoprecipitate Ad2 E3-19K with HLA-A2 (36). In contrast, sites that are spatially remote from residue 56, such as residues 156 and 180 of H-$2K^d$ and the region compromising residues 169 to 182 of HLA-B7 (refer to Fig. 4), were identified as essential for the recognition of these molecules by Ad5 and Ad2, respectively (18, 36). Differences in Ad subtypes, human vs mouse class I molecules, and/or experimental approaches may account for discrepancies with our findings.

Our results showed that E3-19K forms higher affinity complexes (~2.5-fold increase) with HLA-A than with HLA-B molecules. Interestingly, E3-19K interacts only very weakly with HLA-Cw*0304 and showed no affinity for HLA-Cw*0401. To gain insights into how a natural polymorphism may contribute to this binding specificity, we aligned amino acid sequences comprising residues 41 to 61 (see above) of all the reported molecules of the HLA-B and -C loci. The analysis revealed that the stretch comprising residues 47 to 61 (P^{47}R**A**PW**I**EQEG^{56}PEYWD^{61}) is identical with that in HLA-A molecules and is highly conserved in HLA-B molecules. Two polymorphic residues (boldfaced) within that sequence were, however, identified in HLA-C molecules: 1) the A49E mutation that is unique to the HLA-Cw*4 subtype; and 2) the I52V mutation that is absolutely conserved in the HLA-C locus. Based on these comparisons, we suggest that polymorphic residues in the spatial environment around MHC residue 56, including polymorphic residues 49, 52, and those flanking the sequence 47–61, are likely to play an important role in the differential recognition of HLA-A, -B, and -C molecules. To understand why HLA-C molecules interact so differently with E3-19K relative to HLA-A and -B molecules, we introduced a V52I mutation in HLA-Cw*0304, making the sequence 47–61 identical with that of an HLA-B molecule. Results (data not shown) showed that the mixture of E3-19K and HLA-Cw*0304V52I behaved differently on the native gels and gel filtration columns from those involving HLA-B*0702 and -B*0801 (see Fig. 7); no protein smear or fast-eluting peak could be observed. Moreover, no binding response by SPR could be detected at concentrations of E3-19K as high as 2

μM. Thus, despite HLA-Cw*0304V52I being identical with an HLA-B molecule in the aa 47–61 sequence, E3-19K did not recognize HLA-Cw*0304V52I as an HLA-B molecule. This provides convincing evidence that Val^{52} cannot be solely responsible for the extremely weak affinity that E3-19K displays toward HLA-Cw*0304. It is important to note that the results obtained with HLA-Cw*0304 are likely to be representative of HLA-C molecules in general given that the I52V mutation is conserved in the HLA-C locus, but that the A49E mutation is confined to the HLA-Cw*4 subtype. The differential binding specificity displayed by E3-19K toward HLA-A, -B, and -C molecules may be a strategy evolved by Ads to inactivate T cell receptors while avoiding the activation of NK receptors. Other immunomodulatory proteins such as the Kaposi's sarcoma-associated herpes virus K5 protein (37), US2 from human CMV (38), and Nef from HIV-1 (39) were shown to display similar class I binding specificities.

The region of the groove comprising residue 56 is located at the N-terminal end of the α1-helix (see Fig. 4). On the basis of our results indicating that bound peptides are unlikely to be an integral component of the interaction surface in E3-19K/class I complexes, we suggest that the ER lumenal domain of E3-19K interacts with class I molecules by binding away from the binding groove. Such a mode of binding is consistent with previous studies in which we showed that the E3-19K/peptide-deficient HLA-A*1101 complex binds antigenic peptides (20). The E3-19K contact site identified here implies that, in Ad-infected cells, E3-19K is unlikely to compete with the class I assembly proteins calreticulin, tapasin, and ERp57, which are thought to bind at the N-terminal end of the α2-helix (reviewed in Ref. 40). Interestingly, the immunomodulatory US2 protein has been shown to bind at the C-terminal end of the α2 helix of HLA-A2 (41, 42), a site that is also remote from that of the class I assembly proteins. The possibility that peptide-deficient class I molecules sequestered by E3-19K can still interact with class I assembly proteins and mature into peptide-filled molecules would favorably contribute to the immunomodulatory function of E3-19K, given that E3-19K binds more avidly to peptide-filled than peptide-deficient molecules (20) (whether US2 interacts with peptide-deficient class I molecules is less clear (38)). This reasoning suggests that there may be a biological advantage for viral immunomodulatory proteins to occupy a binding site on class I molecules remote from that of class I assembly proteins.

Finally, an analysis of natural polymorphism within the HLA-A locus revealed that residue Arg^{56} is almost exclusively confined to the HLA-A30 and -A31 subtypes. Because Arg^{56} is associated with weak E3-19K binding, it would be informative to examine whether correlations between HLA-A30/-A31 alleles and the resistance or slow progression to Ad infections can be established in populations where these alleles are prevalent or in individuals expressing these alleles. Although susceptibility to infectious diseases is a complex phenomenon, this information could provide valuable insights into the pathogenesis of Ad diseases.

Acknowledgments

We thank Mingnan Chen for discussion and helpful comments on the manuscript. Flow cytometry experiments were conducted at Flow Cytometry Facility of the Biotechnology-Bioservices Center at the University of Connecticut (Storrs, CT). We are grateful to the Core Facilities at Dana-Farber Cancer Institute (Boston, MA) for permission to use their BIAcore 3000 instrument. Gifts of reagents from Drs. P. Cresswell, P. Flomenberg, Y. Jones, P. Sun, and D. Wiley are acknowledged.

Disclosures

The authors have no financial conflict of interest.

References

1. Horwitz, M. S. 1990. Adenoviruses. In *Virology*, 2nd ed. B. N. Fields, D. M. Knipe, R. M. Chanock, M. S. Hirsch, J. L. Melnick, T. P. Monath, and B. Roizman, eds. Raven Press, New York, NY, pp. 1723–1763.
2. Wold, W. S. M., and L. R. Gooding. 1991. Region E3 of adenovirus: a cassette of genes involved in host immunosurveillance and virus-cell interactions. *Virology* 184: 1–8.
3. Horwitz, M. S. 1990. Adenoviruses. In *Virology*, 2nd ed. B. N. Fields, D. M. Knipe, R. M. Chanock, M. S. Hirsch, J. L. Melnick, T. P. Monath, and B. Roizman, eds. Raven Press, New York, NY, pp. 1679–1721.
4. Vasavada, R., K. Eager, G. Barbani-Brodono, A. Caputo, and R. Ricciardi. 1986. Adenovirus type 12 early region 1A proteins repress class I HLA expression in transformed human cells. *Proc. Natl. Acad. Sci. USA* 83: 5257–5261.
5. Rotem-Yehudar, R., M. Groettrup, A. Soza, P. M. Kloetzel, and R. Ehrlich. 1996. LMP-associated proteolytic activities and TAP-dependent peptide transport for class I molecules are suppressed in cell lines transformed by the highly oncogenic adenovirus 12. *J. Exp. Med.* 183: 499–514.
6. Burgert, H.-G., and S. Kvist. 1985. An adenovirus type 2 glycoprotein blocks cell surface expression of human histocompatibility class I antigens. *Cell* 41: 987–997.
7. Burgert, H.-G., and S. Kvist. 1987. The E3/19K protein of adenovirus type 2 binds to the domains of histocompatibility antigens required for CTL recognition. *EMBO J.* 6: 2019–2026.
8. Cox, J. H., J. W. Yewdell, L. C. Eisenlohr, P. R. Johnson, and J. R. Bennink. 1990. Antigen presentation requires transport of MHC class I molecules from the endoplasmic reticulum. *Science* 247: 715–718.
9. Kvist, S., L. Ostberg, H. Persson, L. Philipson, and P. A. Peterson. 1978. Molecular association between transplantation antigens and cell surface antigen in adenovirus-transformed cell line. *Proc. Natl. Acad. Sci. USA* 75: 5674–5678.
10. Bennett, E. M., J. R. Bennink, J. W. Yewdell, and F. M. Brodsky. 1999. Cutting edge: adenovirus E19 has two mechanisms for affecting class I MHC expression. *J. Immunol.* 162: 5049–5052.
11. Lichtenstein, D. L., K. Toth, K. Doronin, A. E. Tollefson, and W. S. M. Wold. 2004. Functions and mechanisms of action of the adenovirus E3 proteins. *Int. Rev. Immunol.* 23: 75–111.
12. Andersson, M., T. Paabo, T. Nilsson, and P. A. Peterson. 1985. Impaired intracellular transport of class I MHC antigens as a possible means for adenoviruses to evade immune surveillance. *Cell* 43: 215–222.
13. Flomenberg, P., V. Piaskowski, R. L. Truit, and J. T. Casper. 1996. Human adenovirus-specific $CD8^+$ T-cell responses are not inhibited by E3-19K in the presence of γ interferon. *J. Virol.* 70: 6314–6322.
14. Rawle, F. C., A. E. Tollefson, W. S. M. Wold, and L. R. Gooding. 1989. Mouse anti-adenovirus cytotoxic T lymphocytes. *J. Immunol.* 143: 2031–2037.
15. Andersson, M., A. McMichael, and P. A. Peterson. 1987. Reduced allorecognition of adenovirus-2 infected cells. *J. Immunol.* 138: 3960–3966.
16. Ginsberg, H. S., U. Lundholm-Beauchamp, R. L. Horswood, B. Pernis, W. S. M. Wold, R. M. Chanock, and G. A. Prince. 1989. Role of early region 3 (E3) in pathogenesis of adenovirus disease. *Proc. Natl. Acad. Sci. USA* 86: 3823–3827.
17. Beier, D. C., J. H. Cox, D. R. Vining, P. Cresswell, and V. H. Engelhard. 1994. Association of human class I MHC alleles with the adenovirus E3/19K protein. *J. Immunol.* 152: 3862–3872.
18. Feuerbach, D., S. Etteldorf, C. Ebenau-Jehle, J.-P. Abastado, D. Madden, and H.-G. Burgert. 1994. Identification of amino acids within the MHC molecule important for the interaction with the adenovirus protein E3/19K. *J. Immunol.* 153: 1626–1636.
19. Flomenberg, P., E. Gutierrez, and K. T. Hogan. 1994. Identification of class I MHC regions which bind to the adenovirus E3-19K protein. *Mol. Immunol.* 31: 1277–1284.
20. Liu, H., W. F. Stafford, and M. Bouvier. 2005. The endoplasmic reticulum lumenal domain of the adenovirus type 2 E3-19K binds to peptide-filled and peptide-deficient HLA-A*1101 molecules. *J. Virol.* 79: 13317–13325.
21. Cox, J. H., J. R. Bennink, and J. W. Yewdell. 1991. Retention of adenovirus E19 glycoprotein in the endoplasmic reticulum is essential to its ability to block antigen presentation. *J. Exp. Med.* 174: 1629–1637.
22. Paabo, S., B. M. Bhat, W. S. M. Wold, and P. A. Peterson. 1987. A short sequence in the COOH-terminus makes an adenovirus membrane glycoprotein a resident of the endoplasmic reticulum. *Cell* 50: 311–317.
23. Severinsson, L., I. Martens, and P. A. Peterson. 1986. Differential association between two human MHC class I antigens and an adenoviral glycoprotein. *J. Immunol.* 137: 1003–1009.
24. Deryckere, F., and H.-G. Burgert. 1996. Early region 3 of adenovirus type 19 (subgroup D) encodes an HLA-binding protein distinct from that of subgroups B and C. 1996. *J. Virol.* 70: 2832–2841.
25. Korner, H., and H.-G. Burgert. 1994. Down-regulation of HLA antigens by the adenovirus type 2 E3/19K protein in a T-lymphoma cell line. *J. Virol.* 68: 1442–1448.
26. Li, L., and M. Bouvier. 2005. Biochemical and structural impact of natural polymorphism in the HLA-A3 superfamily. *Mol. Immunol.* 41: 1331–1344.
27. Bouvier, M., and D. C. Wiley. 1998. Structural characterization of a soluble and partially folded class I major histocompatibility/β_2m heterodimer. *Nat. Struct. Biol.* 5: 377–382.
28. Garboczi, D. N., D. T. Hung, and D. C. Wiley. 1992. HLA-A2-peptide complexes: refolding and crystallization of molecules expressed in *Escherichia coli* and complexed with single antigenic peptides. *Proc. Natl. Acad. Sci. USA* 89: 3429–3433.

29. Kelly, T. J., and A. M. Lewis, Jr. 1973. Use of nondefective adenovirussimian virus 40 hybrids for mapping the simian virus 40 genome. *J. Virol.* 12: 643–652.
30. Sriwanthana, B., T. Hodge, T. D. Mastro, C. S. Dezzutti, K. Bond, H. A. F. Stephens, L. G. Kostrikis, K. Limpakarnjanarat, N. L. Young, S. H. Qari, et al. 2001. HIV-specific cytotoxic T lymphocytes, HLA-A11, and chemokine-related factors may act synergistically to determine HIV resistance in CCR5 Δ32-negative female sex workers in Chiang Rai, Northern Thailand. *AIDS Res. Hum. Retroviruses* 17: 719–734.
31. Wang, R.-F., S. L. Johnston, S. Southwood, A. Sette, and S. A. Rosenberg. 1998. Recognition of an antigenic peptide derived from tyrosinase-related protein-2 by CTL in the context of HLA-31 and -A33. *J. Immunol.* 160: 890–897.
32. Huczko, E. L., W. M. Bodnar, D. Benjamin, K. Sakaguchi, N. Z. Zhu, J. Shabanowitz, R. A. Henderson, E. Appella, D. F. Hunt, and V. H. Engelhard. 1993. Characteristics of endogenous peptides eluted from the class I MHC molecules HLA-B7 determined by mass spectrometry and computer modeling. *J. Immunol.* 151: 2572–2587.
33. Burrows, S. R., S. J. Rodda, A. Suhrbier, H. M. Geysen, and D. J. Moss. 1992. The specificity of recognition of a cytotoxic T lymphocyte epitope. *Eur. J. Immunol.* 22: 191–195.
34. Zappacosta, F., F. Borrego, A. G. Brooks, K. C. Parker, and J. Coligan. 1997. Peptides isolated from HLA-Cw*0304 confer different degrees of protection from natural killer cell-mediated lysis. *Proc. Natl. Acad. Sc. USA* 94: 6313–6318.
35. Sidney, J., M.-F. del Guercio, S. Southwood, V. H. Engelhard, E. Appella, H.-G. Rammensee, K. Falk, O. Rotzschke, M. Takiguchi, R. T. Kubo, et al. 1995. Several HLA alleles share overlapping peptide specificities. *J. Immunol.* 154: 247–259.
36. Flomenberg, P., E. Gutierrez, and K. T. Hogan. 1994. Identification of class I MHC regions which bind to the adenovirus E3-19K protein. *Mol. Immunol.* 31: 1277–1284.
37. Ishido, S., C. Wang, B.-S. Lee, G. B. Cohen, and J. U. Jung. 2000. Downregulation of major histocompatibility complex class I molecules by kaposi's sarcoma-associated herpesvirus K3 and K5 proteins. *J. Virol.* 74: 5300–5309.
38. Gewurz, B. E., E. W. Wang, D. Tortorella, D. J. Schust, and H. L. Ploegh. 2001. Human cytomegalovirus US2 endoplasmic reticulum-lumenal domain dictates association with major histocompatibility complex class I in a locus-specific manner. *J. Virol.* 75: 5197–5204.
39. Cohen, G. B., R. T. Gandhi, D. M. Davis, O. Mandelboim, B. K. Chen, J. L. Strominger, and D. Baltimore. 1999. The selective downregulation of class I major histocompatibility complex proteins by HIV-1 protects HIV-infected cells from NK cells *Immunity* 10: 661–671.
40. Bouvier, M. 2003. Accessory proteins and the assembly of human class I MHC molecules: a molecular and structural perspective. *Mol. Immunol.* 39: 697–706.
41. Gewurz, B. E., R. Gaudet, D. Tortorella, E. W. Wang, H. L. Ploegh, and D. C. Wiley. 2001. Antigen presentation subverted: structure of the human cytomegalovirus protein US2 bound to the class I molecule HLA-A2. *Proc. Natl. Acad. Sci. USA* 98: 6794–6799.
42. Thilo, C., P. Berglund, S. E. Applequist, J. W. Yewdell, H.-G. Ljunggren, and A. Achour. 2006. Dissection of the interaction of the human cytomegalovirus-derived US2 protein with major histocompatibility complex class I molecules. *J. Biol. Chem.* 281: 8950–8957.
43. Li, L., and M. Bouvier. 2004. Structures of HLA-A*1101 complexed with immunodominant nonamer and decamer HIV-1 epitopes clearly reveal the presence of a middle, secondary anchor residue. *J. Immunol.* 172: 6175–6184.